Ultra-incompressible phases of tungsten dinitride predicted from first principles

Hui Wang,[1] Quan Li,[1] Yinwei Li,[1] Ying Xu,[1] Tian Cui,[1] Artem R. Oganov,[2,3] and Yanming Ma[1,*]

[1]*National Laboratory of Superhard Materials, Jilin University, Changchun 130012, People's Republic of China*
[2]*Department of Geosciences and New York Center for Computational Science, Stony Brook University, Stony Brook, New York 11794, USA*
[3]*Department of Geology, Moscow State University, 119899 Moscow, Russia*
(Received 26 November 2008; published 27 April 2009)

Using *ab initio* evolutionary methodology for crystal structure prediction, we have found two ultra-incompressible hexagonal structures of $P6_3/mmc$ and P-$6m2$ of WN_2, which are energetically much superior to previously proposed baddeleyite- and cotunnite-type structures and stable against decomposition into a mixture of $W+N_2$ or $WN+1/2N_2$. The calculated large bulk modulus (e.g., 411 GPa) and high hardness (36.8 GPa for $P6_3/mmc$ and 36.6 GPa for P-$6m2$) reveal that they are ultra-incompressible and hard materials. The ultra-incompressibility is attributed to a staking of N-W-N "sandwiches" layers linked by strong covalent N-N single bonding. Thermodynamic study suggests that these phases are synthesizable at above 30 GPa.

I. INTRODUCTION

Solid nitrides have been the subject of intense experimental and theoretical studies due to their technological and fundamental importance.[1–3] Transition metals were previously known to hardly form nitrides with high nitrogen content. Until recently, platinum-metal (e.g., Pt, Ir, Os, and Pd) dinitrides were successfully synthesized under extreme conditions of high pressure and temperature.[4–7] Except for PdN_2 all these nitrides can be quenched and stabilized to ambient conditions and possess outstanding mechanical properties (e.g., an ultrahigh bulk modulus of 428 GPa for IrN_2). The anomalously low compressibility of these nitrides, comparable to that of *c*-BN, suggests that they are potential (super)hard materials. The crystal structures for these nitrides have been extensively studied[8–14] and the consensus appears to be that the origin of their incompressibility derives mainly from the directional bonding of interstitial dinitrogen. Are there other (super)hard transitional metal dinitrides? Results are worth the effort. Here, the crystal structures of WN_2 were extensively explored over a wide range of pressures.

To date, WN_2 has not been synthesized in crystalline form. For a long time it has been theoretically suggested to adopt a fluorite-type structure.[15] However, Peter *et al.*[16] recently proposed two structures of baddeleyite and cotunnite types, which are energetically much superior to the fluorite-type structure and exhibit ultrahigh bulk modulus (e.g., 408 GPa for cotunnite WN_2). Interestingly, these structures do not contain the dinitrogen, in contrast to the known structures of the platinum-metal dinitrides. The calculated pressure-temperature phase diagram suggested that these two crystalline forms can be synthesized at pressure above 31 GPa at 2800 K.[16] However, the proposed two structures were based on educated guesses from structures known for other materials. There is a possibility that hitherto unsuspected structures are stable instead and the picture of chemical bonding in this nitride will change fundamentally. Therefore, we have extensively explored the crystal structures of WN_2 over a wide range of pressures (0–60 GPa) using a newly developed approach,[17–20] merging *ab initio* simulations and a specifically developed evolutionary algorithm for crystal structure prediction. This method has been very successful in predicting the unknown structures with the only information of *chemical compositions*.[21–26] A stable hexagonal $P6_3/mmc$ structure and a metastable P-$6m2$ structure both possessing dinitrogen are predicted and energetically much favorable than those of the baddeleyite- and cotunnite-type structures. The two structures are ultra-incompressible and have not been reported in any other compounds.

II. COMPUTATIONAL DETAILS

The evolutionary variable-cell simulations were performed at 0 and 60 GPa with systems containing 1, 2, 3, and 4 f.u. in the simulation cell using the USPEX code.[17–20] The underlying *ab initio* calculations were carried out using density-functional theory within both the generalized gradient approximation[27] (GGA) and the local-density approximation[28] (LDA) as implemented in the Vienna *ab initio* simulation package.[29] The all-electron projector augmented wave[30,31] (PAW) method was adopted with the PAW potential of the metal atoms including *d* electrons as valence states. The cutoff energy (520 eV) for the expansion of the wave function into plane waves and Monkhorst-Pack *k* points meshes were chosen to ensure that all the structures are well converged to better than 1 meV/f.u.[32] During the subsequent geometrical optimization, all forces on atoms were converged to less than 0.001 eV/Å and the total stress tensor was reduced to the order of 0.01 GPa. Elastic constants were calculated by the strain-stress method and the polycrystalline bulk modulus and shear modulus were thus derived from the Voigt-Reuss-Hill averaging scheme.[33]

III. RESULTS AND DISCUSSION

We obtained the hexagonal $P6_3/mmc$ and P-$6m2$ structures at both pressures from evolutionary structural search. Specifically, the hexagonal $P6_3/mmc$ structure is derived at the eleventh generation (15 structures per generation) in the 2 f.u. simulation at 0 GPa and the P-$6m2$ structure can be
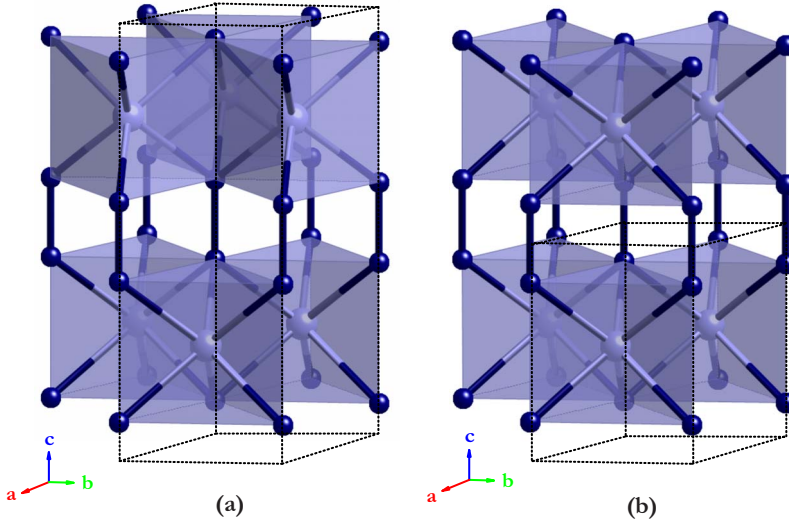
FIG. 1. (Color online) Polyhedral views of the (a) $P6_3/mmc$ and (b) P-$6m2$ structures. The dark dot lines denote the unit cells and the large and small spheres represent W and N atoms, respectively. The $P6_3/mmc$ structure contains two f.u. per cell with W occupying the Wyckoff $2d$ ($\frac{2}{3}$, $\frac{1}{3}$, and $\frac{1}{4}$) sites, and N sitting at $4e$ $(0,0,z)$ positions, with $z=0.09016$. For the P-$6m2$ structure, there is 1 f.u. per cell, W and N atoms occupying the Wyckoff $1f$ ($\frac{2}{3}$, $\frac{1}{3}$, and $\frac{1}{2}$) and $2g$ $(0,0,z)$ with $z=0.18133$ positions, respectively.

arrived at the eighth generation (15 structures per generation) in the 1 f.u. simulation at 0 GPa. Polyhedral views of both structures (Fig. 1) reveal an intriguing N-W-N sandwiches stacking order. In both structures, N atoms form hexagonal planes alternatively. In every pair of congruent planes, there are edge-sharing trigonal prisms which contain W atoms and form the sandwiches layer. The W atoms adopt a hexagonal close-packed (hcp) pattern $ABAB$ for $P6_3/mmc$ and a simple hexagonal (sh) arrangement AA for P-$6m2$. Interestingly, the sandwich-type stacking in these two structures seems to be similar to that in MoS$_2$ structure.[34] However the S-S distance (3.66 Å) between the S-Mo-S sandwiches in MoS$_2$ structure is very large and approximately equals to the sum of two radii of S^{2-} ions. The only attractive forces between the sandwiches in MoS$_2$ structure are weak van der Waals interactions, and they can easily slip as in graphite. On the contrary, the N-N bond lengths in these two polymorphs (Table I) are close to the value of ~1.4 Å observed in OsN$_2$ and PtN$_2$,[4,6] consistent with a typical N-N single bond (1.45 Å in N$_2$H$_4$) but much longer than the double bond (1.21 Å for N$_2$F$_2$) and triple bond (1.09 Å for N$_2$). Previous studies[13] have shown that an important stabilizing effect in platinum-metal dinitride comes from the strong covalent N-N bonding, which is comparable to the C-C bonding in diamond. Here, by reinforcing the links of the N-W-N sandwiches layers, this strong covalent N-N bonding also provides a strengthening effect to make the material possess very low compressibility (*ut infra*). These two structures do not have analogs in other compounds; however, the $P6_3/mmc$ and P-$6m2$ struc-

tures can be viewed as NiAs-type and WC-type structures with dinitrogen occupying the Ni and C positions, respectively. The dynamical stabilities of the two structures have been confirmed by analysis of the calculated phonon-dispersion curves in the pressure range of 0–60 GPa. No any imaginary phonon frequency was found in the whole Brillouin zone.

The enthalpy curves for different structures relative to $P6_3/mmc$ are shown in Fig. 2(a). It can be clearly seen that the two predicted structures with very similar enthalpies are much more favorable than earlier structures in the whole pressure range. It is important to note that the enthalpy difference (per f.u.) of P-$6m2$ relative to $P6_3/mmc$ is only 1.3 meV (10.5 meV) at ambient pressure and increases linearly with pressure up to 10.5 meV (19.3 meV) at 60 GPa within GGA (LDA), as shown in Fig. 2(b). This behavior is mainly originated from the difference in PV works [Fig. 2(c)] or volumes between the two structures. Note that the hcp arrangement of W atoms lead to a more economic space filling in $P6_3/mmc$ than that of P-$6m2$ with W atoms possessing the sh pattern. As a result, P-$6m2$ structure has a larger volume to sacrifice its enthalpy.

The thermodynamic stability of the two structures at ambient pressure with respect to the decomposition was quantified in terms of the formation enthalpies of two reaction routes:

$$\Delta H_{f(\mathrm{I})} = H_{\mathrm{WN_2}} - (H_{\mathrm{W}} + H_{\mathrm{N_2}}), \qquad (1)$$

TABLE I. Calculated equilibrium lattice parameters, a_0 (Å) and c_0 (Å), equilibrium volume per f.u., V_0 (Å^3), bonding length of dinitrogen $d_{\mathrm{N\text{-}N}}$ (Å), formation enthalpies of the two reaction routes $H_{f(\mathrm{I})}$ (meV) and $H_{f(\mathrm{II})}$ (meV), elastic constants c_{ij} (GPa), bulk modulus B (GPa), and shear modulus G (GPa).

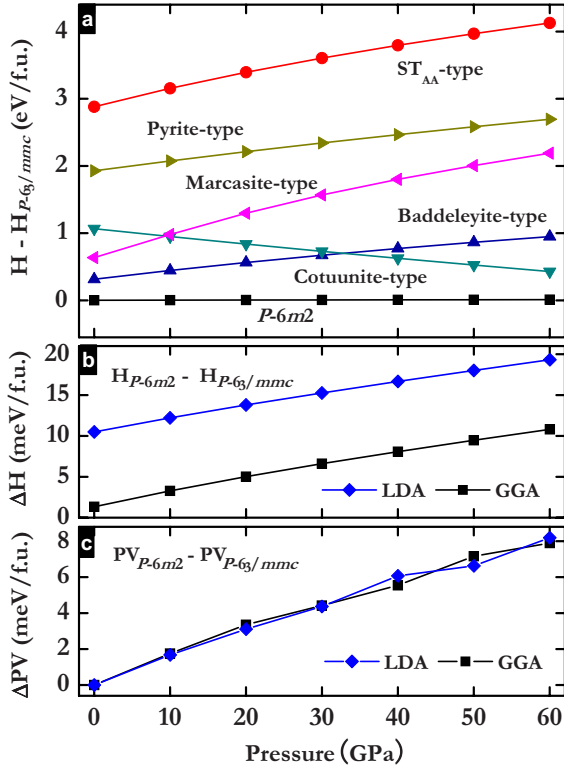| Phases		a_0	c_0	V_0	$d_{\mathrm{N\text{-}N}}$	$d_{\mathrm{W\text{-}N}}$	$H_{f(\mathrm{I})}$	$H_{f(\mathrm{II})}$	c_{11}	c_{33}	c_{44}	c_{12}	c_{13}	B	G
$P6_3/mmc$	GGA	2.934	7.790	29.035	1.405	2.102	−942.4	−477.0	579	973	233	195	211	364	228
	LDA	2.887	7.711	27.821	1.383	2.075	−2207.3	−979.3	642	1078	262	217	252	411	252
P-$6m2$	GGA	2.928	3.916	29.069	1.420	2.101	−941.1	−476.7	588	973	232	191	206	364	231
	LDA	2.881	3.875	27.850	1.397	2.074	−2196.8	−986.8	654	1082	260	213	248	412	255

FIG. 2. (Color online) (a) Enthalpies (relative to the $P6_3/mmc$ structure within GGA) for various structures as a function of pressure. The marcasite structure for IrN$_2$ (Ref. 13), the pyrite and ST$_{AA}$ structures for PtN$_2$ (Ref. 14) are also considered for comparison. (b) Enthalpy of P-6m2 relative to $P6_3/mmc$. (c) PV works of P-6m2 relative to $P6_3/mmc$.

$$\Delta H_{f(\text{II})} = H_{\text{WN}_2} - \left(H_{\text{WN}} + \tfrac{1}{2} H_{\text{N}_2} \right), \qquad (2)$$

The body-centered-cubic W, NiAs-type WN, and α phase N$_2$ were chosen as the reference phases. Results obtained by the two reaction routes within both GGA and LDA have demonstrated the stability against the decomposition into the mixture of W+N$_2$ or WN+1/2N$_2$ (Table I). Syntheses of these two polymorphs are thus desirable. However, one must take a caution in the experiment in view of the existence of large energy barriers in the formation of nitrides. For example, the predicted formation pressures within GGA for the IrN$_2$ and PtN$_2$ are 17 and 15 GPa, respectively, while in experiments, the synthesis pressures for both materials approach 50 GPa.[4–6] It is suggested that for the 5d transition-metal dinitrides,[4–7] GGA predicts formation pressures in $\sim$30 GPa lower than the experimental ones. Thus, syntheses of the two polymorphs could be expected above 30 GPa.

The partial densities of states of the two phases were plotted in Fig. 3. Both phases are semiconductors characterized by energy gaps of $\sim$1.2 eV for GGA ($\sim$1.4 eV for LDA). Since density-functional calculations typically underestimate energy gap within 30%–50%, the true band gap might be located in the region of 1.6–2.1 eV for optical applications. It was also suggested that W 5d orbital has a significant hybridization with N 2p orbital, signifying the strong W-N covalent bonding nature within the sandwiches layers, which
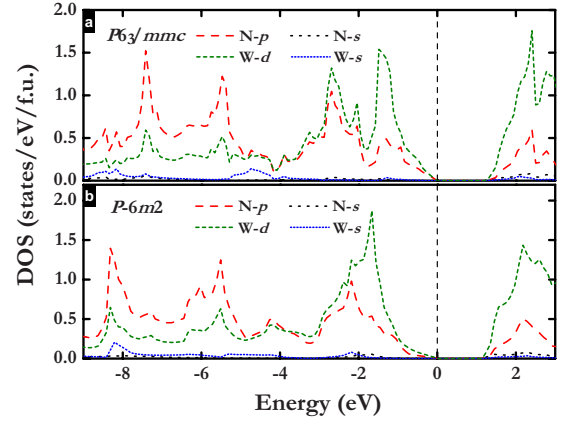

FIG. 3. (Color online) Partial densities of states of the $P6_3/mmc$ structure (a) and the P-6m2 structure (b). Vertical dashed line is the Fermi energy.

has been further confirmed by our simulated electron-density distributions.

The elastic constant c_{33} measures the c-direction resistance to linear compression. The large c_{33} (973 GPa for GGA) in the two structures manifests that the c-axial direction is extremely stiff and the anisotropic factor, $A_{\text{shear}} = 2c_{44}/(c_{11}-c_{12}) \approx 1.2$, indicates an anisotropy in shear. Both phases exhibit very high bulk modulus (364 GPa within GGA) indicating ultra-incompressible structural nature. For the partially covalent transition-metal-based hard materials, the polycrystalline shear modulus has been considered as very important parameter, governing the indentation hardness.[35] Remarkably, the calculated polycrystalline shear modulus are very large, 228 GPa for $P6_3/mmc$ and 231 GPa for P-6m2 within GGA. Thus, the two phases are expected to withstand shear strain to a large extent and are harder than many known hard materials (such as TiN, ZrC, and Al$_2$O$_3$).[35] Indeed, the estimated theoretical Vickers hardness for the $P6_3/mmc$ and P-6m2 structures by using Simunek's method[36] are 36.8 GPa and 36.6 GPa, respectively, which beyond the hardness values of α-SiO$_2$ (30.6 GPa) and β-Si$_3$N$_4$ (30.3 GPa).[37] We attribute the excellent mechanical properties of the two phases to the stacking of N-W-N sandwiches layers linked through strong covalent N-N single bonds.

IV. CONCLUSION

In summary, we have predicted two ultra-incompressible hexagonal $P6_3/mmc$ and P-6m2 phases of WN$_2$ through the developed evolutionary algorithm. The strong covalent N-N single bonding in these two phases analogizing to the newly synthesized platinum-metal dinitrides is one of the key to understand the anomalously low compressibility. These two polymorphs have been demonstrated to be synthesizable at high pressure. Despite the low x-ray scattering contribution of the N atoms relative to the W atoms, the two hexagonal phases with W atoms form hcp and sh sublattices will be easy to detect.

*Author to whom correspondence should be addressed; mym@jlu.edu.cn

[1] S. H. Jhi, J. Ihm, S. G. Louie, and M. L. Cohen, Nature (London) **399**, 132 (1999).

[2] E. Horvath-Bordon, R. Riedel, A. Zerr, P. F. McMillan, G. Auffermann, Y. Prots, W. Bronger, R. Kniep, and P. Kroll, Chem. Soc. Rev. **35**, 987 (2006).

[3] A. Zerr, G. Miehe, and R. Riedel, Nat. Mater. **2**, 185 (2003).

[4] E. Gregoryanz, C. Sanloup, M. Somayazulu, J. Badro, G. Fiquet, H. K. Mao, and R. J. Hemley, Nat. Mater. **3**, 294 (2004).

[5] J. C. Crowhurst, A. F. Goncharov, B. Sadigh, C. L. Evans, P. G. Morrall, J. L. Ferreira, and A. J. Nelson, Science **311**, 1275 (2006).

[6] A. F. Young, C. Sanloup, E. Gregoryanz, S. Scandolo, R. J. Hemley, and H. K. Mao, Phys. Rev. Lett. **96**, 155501 (2006).

[7] J. C. Crowhurst, A. F. Goncharov, B. Sadigh, J. M. Zaug, D. Aberg, Y. Meng, and V. B. Prakapenka, J. Mater. Res. **23**, 1 (2008).

[8] R. Yu, Q. Zhan, and X. F. Zhang, Appl. Phys. Lett. **88**, 051913 (2006).

[9] A. F. Young, J. A. Montoya, C. Sanloup, M. Lazzeri, E. Gregoryanz, and S. Scandolo, Phys. Rev. B **73**, 153102 (2006).

[10] J. von Appen, M. W. Lumey, and R. Dronskowski, Angew. Chem., Int. Ed. **45**, 4365 (2006).

[11] Z. W. Chen, X. J. Guo, Z. Y. Liu, M. Z. Ma, Q. Jing, G. Li, X. Y. Zhang, L. X. Li, Q. Wang, Y. J. Tian, and R. P. Liu, Phys. Rev. B **75**, 054103 (2007).

[12] Y. X. Wang, M. Arai, T. Sasaki, and C. Z. Fan, Phys. Rev. B **75**, 104110 (2007).

[13] R. Yu, Q. Zhan, and L. C. De Jonghe, Angew. Chem., Int. Ed. **46**, 1136 (2007).

[14] D. Aberg, B. Sadigh, J. Crowhurst, and A. F. Goncharov, Phys. Rev. Lett. **100**, 095501 (2008).

[15] F. P. L. G. R. J. Meyer, E. Pietsch, and M. Beche-Goehring, *Gmelins Handbuch der Anorganischen Chemie* (Springer, Berlin, 1933), p. 154.

[16] P. Kroll, T. Schroter, and M. Peters, Angew. Chem., Int. Ed. **44**, 4249 (2005).

[17] C. W. Glass, A. R. Oganov, and N. Hansen, Comput. Phys. Commun. **175**, 713 (2006).

[18] A. R. Oganov and C. W. Glass, J. Chem. Phys. **124**, 244704 (2006).

[19] A. R. Oganov, C. W. Glass, and S. Ono, Earth Planet. Sci. Lett. **241**, 95 (2006).

[20] A. R. Oganov and C. W. Glass, J. Phys.: Condens. Matter **20**, 064210 (2008).

[21] Y. M. Ma, A. R. Oganov, and C. W. Glass, Phys. Rev. B **76**, 064101 (2007).

[22] Y. M. Ma, A. R. Oganov, and Y. Xie, Phys. Rev. B **78**, 014102 (2008).

[23] G. Y. Gao, A. R. Oganov, A. Bergara, M. Martinez-Canales, T. Cui, T. Iitaka, Y. M. Ma, and G. T. Zou, Phys. Rev. Lett. **101**, 107002 (2008).

[24] Y. Ma, A. R. Oganov, Z. Li, Y. Xie, and J. Kotakoski, Phys. Rev. Lett. **102**, 065501 (2009).

[25] A. R. Oganov, J. Chen, C. Gatti, Y. Ma, Y. Ma, C. W. Glass, Z. Liu, T. Yu, O. O. Kurakevych, and V. L. Solozhenko, Nature (London) **457**, 863 (2009).

[26] Y. Ma, M. Eremets, A. R. Oganov, Y. Xie, I. Trojan, S. Medvedev, A. O. Lyakhov, M. Valle, and A. V. Prakapenka, Nature (London) **458**, 182 (2009).

[27] J. P. Perdew and Y. Wang, Phys. Rev. B **45**, 13244 (1992).

[28] D. M. Ceperley and B. J. Alder, Phys. Rev. Lett. **45**, 566 (1980).

[29] G. Kresse and J. Furthmüller, Phys. Rev. B **54**, 11169 (1996).

[30] P. E. Blöchl, Phys. Rev. B **50**, 17953 (1994).

[31] G. Kresse and D. Joubert, Phys. Rev. B **59**, 1758 (1999).

[32] Especially, for the $P6_3/mmc$ and P-$6m2$ structures with very similar total energies, the cutoff energy of 1000 eV and the k-point sampling scheme, $15 \times 15 \times 5$ and $15 \times 15 \times 10$, were adopted to give convergence of the total energies better than 0.1 meV/f.u. The effect of k-point sampling on the total-energy calculations had been eliminated by the carefully additional check using very large k-point sets of $30 \times 30 \times 10$ and $30 \times 30 \times 20$. During the subsequent geometrical optimization, all forces on atoms were converged to less than 0.001 eV/Å and the total stress tensor was reduced to the order of 0.001 GPa.

[33] R. Hill, Proc. Phys. Soc. London **65**, 349 (1952).

[34] E. D. Bodie and S. M. Ho, *Structure and Chemistry of Crystalline Solids* (Springer, New York, 2006), p. 139.

[35] V. V. Brazhkin, A. G. Lyapin, and R. J. Hemley, Philos. Mag. A **82**, 231 (2002).

[36] A. Simunek, Phys. Rev. B **75**, 172108 (2007). In the hardness calculations for the two hexagonal phases, the atomic data r_W =1.41, r_N=0.88, Z_W=6, and Z_N=5 and the calculated bond lengths and equilibrium volumes within the GGA (Table I) have been used.

[37] F. Gao, J. He, E. Wu, S. Liu, D. Yu, D. Li, S. Zhang, and Y. Tian, Phys. Rev. Lett. **91**, 015502 (2003).